JMEPEG (2018) 27:4548–4560
https://doi.org/10.1007/s11665-018-3555-8

1059-9495/$19.00

The Influence of Galvanizing Parameters on the Structural Development of Zn-Al-Based Coatings

E.L. Tiron, A. Crisan, T. Bedő, M. Stoicanescu, M.A. Pop, and D. Cristea

(Submitted August 20, 2017; in revised form July 25, 2018; published online August 10, 2018)

The evolution of some layers' characteristics, deposited by galvanization, was monitored according to the technological parameters of the process. Two types of alloys from the Zn-Al and Zn-Al-Ti-B systems were used for deposition. The structure of the deposited layers was analyzed by optical and electron microscopy. The chemical composition, phases and compounds in the structures were identified. The mechanical properties of the structural constituents of the layers were determined by nanoindentation. These techniques highlighted the typical non-uniformities in terms of composition and properties in the layers, mainly due to the diffusion and distribution of iron from the steel substrate in the deposited layers. The evaluation of iron diffusion in the deposited layer was done by differential thermal analysis. The values of the critical temperatures (melting temperature, eutectic temperature and solidification temperature) were correlated with the parameters used during deposition. It was observed that the structure of the coatings is layered, with a specific order from the steel substrate to the edge. In these layers, the constituents are mixtures of soft solid solutions of Al in Zn (η and β) and hard intermetallic compounds. Moreover, increasing the immersion time in the galvanizing bath and the bath temperature leads to an increase in iron diffusion in the coating layer, which contributes to lower coating thickness, thus reducing its durability in operation.

Keywords chemical composition, galvanizing temperature, immersion time, thermal analysis, Zn-based alloys

1. Introduction

Hot-dip galvanizing is one of the most effective methods of protecting ferrous materials against corrosion. In this technique, the ferrous substrate is immersed in a bath of molten zinc and, as a result, it is covered with a layer of zinc with an average thickness of the order of a few tens of microns (Ref 1).

The galvanizing bath has a significant influence on the structure and performance characteristics of the coating (Ref 2, 3). A series of studies in the field have determined that in order to obtain higher quality products, an appropriate adjustment of the following main parameters is required: the chemical composition of the steel substrate, the chemical composition of the zinc alloys, the galvanizing temperature and the immersion time in the zinc alloy bath (Ref 1, 4-7). The chemical composition of the steel substrate is a determining factor on the quality of the coating, considering that it can influence the growth rate of the different layers of zinc during galvanization (Ref 1, 4, 5). Moreover, it has been found that, depending on the geometry and composition of the steel substrate, the growth of the zinc coating can be controlled both by the chemical composition of the zinc bath and by the physical and operational parameters (Ref 8).

In the coating material, as long as it is in liquid state, an active process of diffusion of iron and other ferrous alloy elements occurs. This in turn depends on all the parameters involved in the galvanization, and it eventually decisively determines the structure and properties of the coating (Ref 1, 9). The quantitative assessment of the effect of some galvanizing parameters on this diffusion process is difficult. Generally, indirect assessments can be made, through structural analyses highlighting phases which are specific to the Zn-Fe equilibrium system, or to more complex Zn-Fe-Al systems. In the same time, reliable chemical analyses offer information that highlights the presence of Fe atoms and other elements in the coating. In this context, an assessment regarding changes in the composition of the galvanizing layer, following the diffusion of elements from the ferrous substrate, can be more accurately obtained from specific temperatures, related to melting-solidification processes, determined by thermal analysis. Since the thermal analysis stability is measured using relatively low heating–cooling speeds, and if the layer is in liquid state, the diffusion process can continue, modifying its composition compared to the previous one. To reproduce this effect in real life, we have opted to maintain the deposition for a period prolonged to one hour. Thus, there can be assessed the effect of parameters such as the composition of the steel substrate, the composition of the galvanizing bath and the galvanization temperature on the melting—solidification temperatures of the deposited layer.

2. Experimental Procedure

The study was conducted on two groups of Zn-based galvanizing alloys, Zn-Al and Zn-Al-Ti-B, respectively. To assess the effect of the galvanization temperature and of the chemical composition of the galvanization alloy on the diffusion phenomena, samples were deposited at 450, 460, 470 and 480 °C with an immersion period of 60 min (Fig. 1a). The effect of the immersion period on the diffusion phenomena

E.L. Tiron, A. Crisan, T. Bedő, M. Stoicanescu, M.A. Pop, and **D. Cristea**, Materials Science Department, Transilvania University of Brasov, Brasov, Romania. Contact e-mail: tiron_lacramioara@yahoo.com.

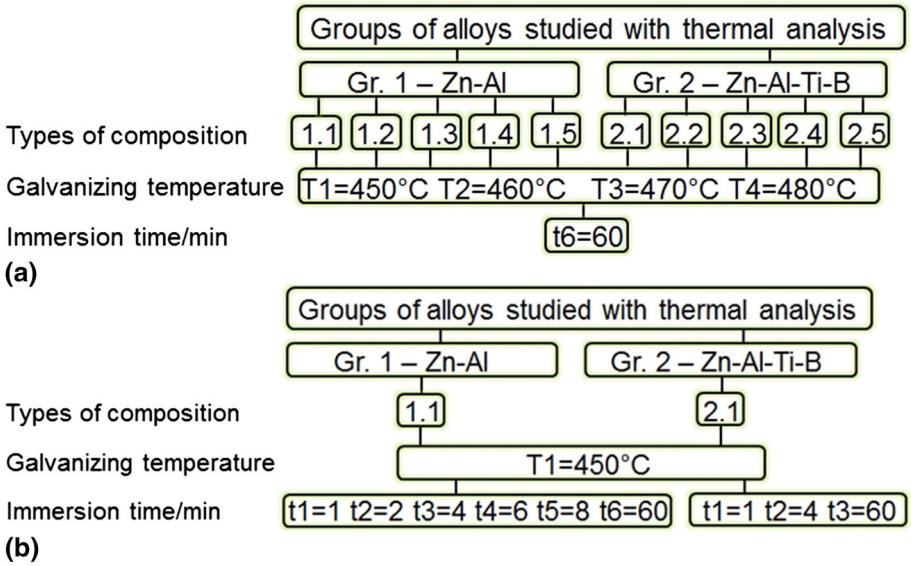

Fig. 1 (a) Assessment on the galvanizing temperature and of the chemical composition of the galvanization alloy regarding the diffusion phenomena; (b) assessment on the immersion time effect on the diffusion phenomena

Table 1 Chemical composition of Zn-Al alloys

	Chemical composition, %							
Alloy set 1	**Pb**	**Mg**	**Al**	**Cd**	**Fe**	**Sn**	**Cu**	**Zn**
1.1	0.0008	0.001	0.868	0.000	0.007	0.0014	0.069	99.053
1.2	0.0006	0.001	0.713	0.000	0.005	0.0021	0.065	99.213
1.3	0.0007	0.001	3.790	0.000	0.011	0.0018	0.056	96.139
1.4	0.0008	0.001	3.994	0.000	0.012	0.0016	0.045	95.946
1.5	0.007	0.001	5.276	0.001	0.015	0.0020	0.038	94.668

was assessed on samples deposited at 450 °C, with various immersion periods, as shown in Fig. 1(b).

The alloys of the first group, from the Zn-Al system, with the chemical composition shown in Table 1, were deposited on a steel substrate (type 1) having the chemical composition (in wt.%): Fe—98.66; C—0.035; Mn—0.592; P—0.024; Cr—0.019; Ni—0.018; Al—0.018; N—0.325, traces of other elements.

The alloys from the second group, from the Zn-Al-Ti-B system, with the chemical composition shown in Table 2 were deposited on a steel substrate (type 2) having the composition (in wt.%): Fe—99.56; C—0.022; Mn—0.228; P—0.013; Cr—0.032; Ni—0.022; Al—0.012; Mo—0.017; Cu—0.037; N—0.024, traces of other elements.

The depositions were assessed in terms of thickness, morphology, phase chemical composition and mechanical properties. The thickness of the deposited layers was examined in cross section, by optical microscopy, with average values between 35 and 112 μm for Zn-Al alloys and between 74 and 114 μm for Zn-Al-Ti-B alloys. The coating morphology was analyzed by optical microscope (Nikon MA100) and scanning electron microscope (SEM, Hitachi, S3400N and Vega3 Tescan, using high vacuum).

Nanoindentation measurements were taken on selected samples, using a CSM Instruments/Anton Paar NHT2 module, equipped with a diamond Berkovich indenter.

Thermal analysis was performed using the DSC 200 F3 Maia/STA 449F3 differential scanning calorimeter. Differential scanning calorimetry measures the thermal effect differences between the sample and a reference material, while undergoing a controlled program of temperature variation. Small samples (∼ 80 mg), containing both a layer portion and a substrate one,

Table 2 Chemical composition of Zn-Al-Ti-B alloys

	Chemical composition, %									
Alloy Set 2	Pb	Mg	Al	Cd	Fe	Ti	B	Sn	Cu	Zn
2.1	0.0139	0.001	1.107	0.003	0.003	0.055	0.011	0.0014	0.026	98.820
2.2	0.0120	0.001	2.137	0.003	0.005	0.430	0.080	0.0008	0.014	97.319
2.3	0.0221	0.001	2.198	0.003	0.005	0.430	0.080	0.0035	0.034	97.223
2.4	0.0181	0.001	2.518	0.003	0.003	0.500	0.100	0.0017	0.027	96.828
2.5	0.0103	0.001	2.559	0.003	0.003	0.510	0.100	0.0005	0.013	96.802

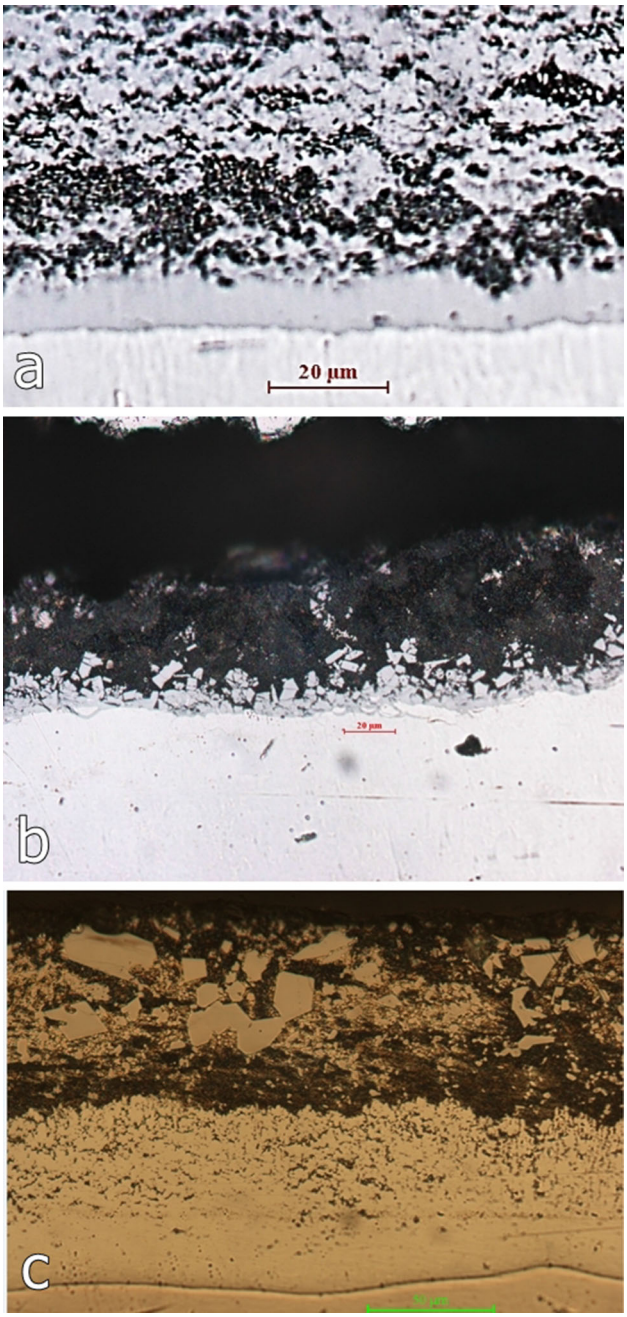

Fig. 2 Microstructure of the deposited layers: (a) alloy 1.5 sample at a temperature of 450 °C immersed in the bath for 60 min., on steel type 1; (b) alloy 1.1 sample at a temperature of 450 °C immersed in the bath for 60 min., on steel type 1; (c) alloy 2.2 sample at a temperature of 470 °C immersed in the bath for 60 min., on steel type 2

were placed inside aluminum crucibles and heated/cooled at a speed of 5 °C min^{-1}, in nitrogen atmosphere during heating and in air during cooling.

3. Results and Discussion

3.1 Morphology and Chemical Composition

The coatings exhibit a typical layered appearance, as it can be observed in Fig. 2. The first layer formed on the steel substrate is very thin (hardly visible). The second layer of greater thickness is compact, with columnar shaped crystals. The third layer, with the highest thickness, is a mixture of phases and compounds. The appearance of these areas varies depending on the conditions of the galvanic coating. Thus, it can be seen that at different Al contents in the galvanizing alloy both the thickness of the previously mentioned layers and the appearance of the structural grains change: the thickness of the second layer is higher at a higher Al content (Fig. 2a and b); at lower Al contents, the crystals of the second layer have a more pronounced polyhedral form (Fig. 2b). In the case of the 2.2 alloy type, the thickness of the structural layers differs greatly from those of the alloy group 1 (Fig. 2c compared to Fig. 2a and b). A cause of these significant differences could be, among others, the different chemical composition of the substrate.

Moreover, the compounds that appear in the structure can have a varied distribution, depending on the actual deposition conditions. According to the Al-Zn equilibrium diagram (Fig. 3, Ref 11), for aluminum contents in the galvanizing alloy up to 5.276% (the maximum Al content of the galvanizing alloys presented herein) the structure of the coating layer should be composed of a mixture of α and η solid solutions, at ambient temperature. For aluminum contents up to 1.00%, the structure after solidification is composed of η solid solution of Al in Zn (with hexagonal lattice). Further cooling to 275 °C precipitates the solid solution β (face-centered cubic) richer in Al. At this temperature, the structure changes as a result of a eutectoid reaction, the β solid solution turns into α solid solution (face-centered cubic). The ratio of α increases with the increase in the Al content.

The diffusion of iron from the steel substrate into the coating along with the presence of other elements in the composition of the galvanizing alloy has very important effects on the structural constituents of the layer, which determine the existence of these separate areas. Although the solubility of Fe in Zn is very limited, due to its presence a series of intermetallic compounds could appear. At the galvanizing temperatures (450-480 °C), according to the binary Fe-Zn diagram, the $\Gamma 1$ and $\Gamma 2$ intermetallic compounds, and the δ and

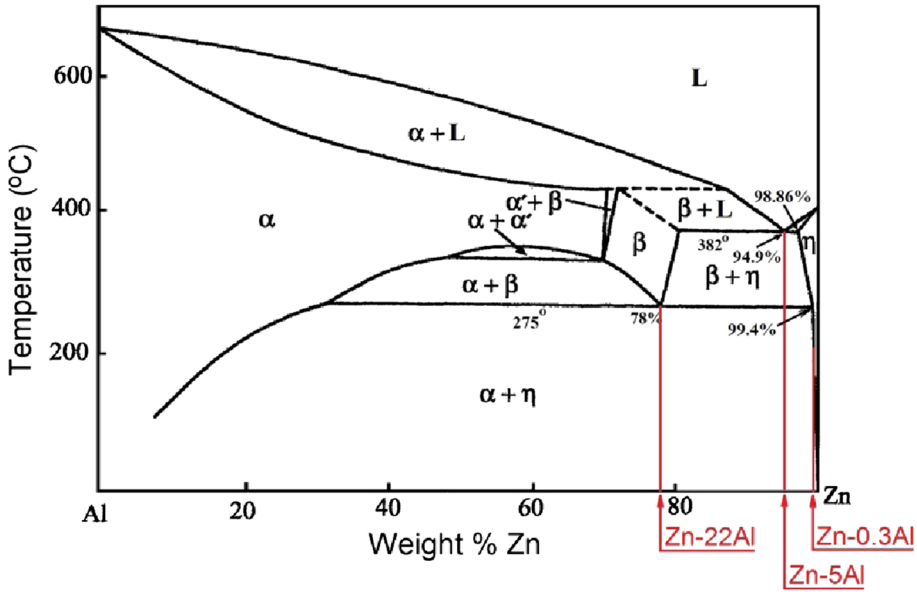

Fig. 3 Binary Zn-Al phase diagram (Ref 11)

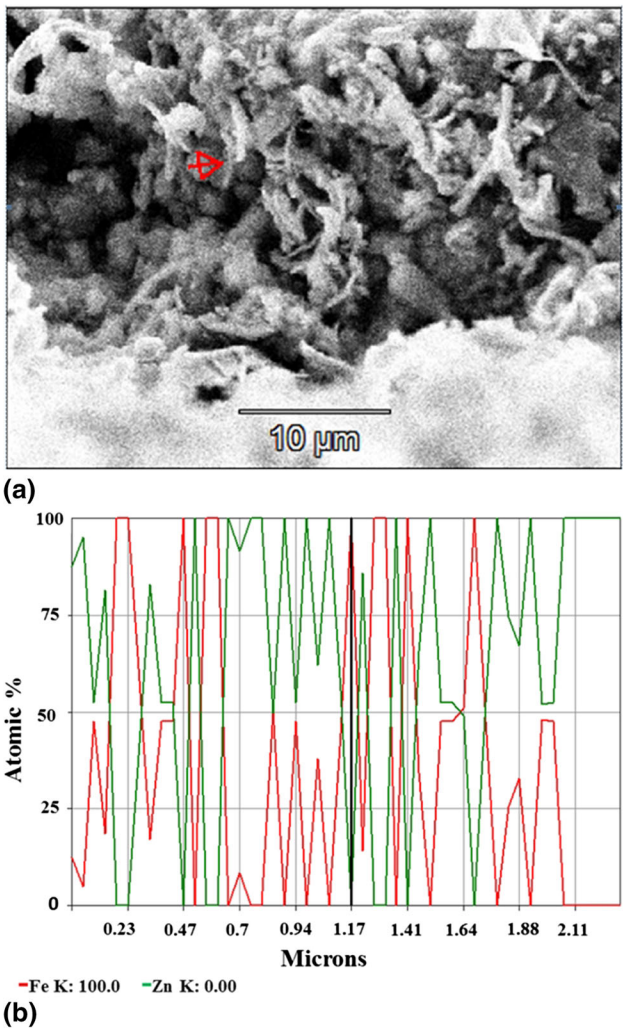

Fig. 4 (a) The microstructure of the deposited layer for the sample 1.5 galvanized at a temperature of 480 °C and immersed in the bath for 60 min. by electron microscope (accelerating voltage: 15 kV); (b) the variation of the composition in the arrow marked area (binary compound)

ξ solid solutions may form in the galvanized layer, due to the diffusion of iron (Ref 12).

The existence of some phases and compounds with different chemical compositions mainly due to the diffusion of iron from the substrate in the layer is presented hereinafter. In Fig. 4 and 5, the chemical composition for certain regions, marked by arrows, is shown. By drawing a vertical line in Fig. 4(b) and 5(b), it is possible to determine the chemical composition at each point starting from the end of the arrows to their peaks. In both cases, important variations in the chemical composition can be observed, for the identified elements. For example, in Fig. 4 it is observed that on a three-micron range, the Fe and Zn percentages of the analyzed grain vary between 0 and 100% for each element. The average composition over the entire length of the analyzed area is as follows: Fe: 50.23% and Zn: 49.77%, in atomic percent. This is a nearly stoichiometric Fe-Zn type compound.

In the second case (Fig. 5), an analysis carried out on a larger area reveals the presence of other elements. The concentrations of the detected elements vary within wide limits (Fig. 5b). The average composition of the studied area is as follows: 18.15% Al, 5.66% Fe, 70.70% Zn and 5.49% Sn, in atomic percent.

Comparing the chemical composition results obtained from EDX spectra in different zones of the coatings, shown in Fig. 6 and Table 3, certain observation can be made. In Fig. 6(a) and (b), very different compositions of the studied areas in the layers can be observed. As the analyzed areas are closer to the steel substrate, the Fe content is higher. At the same time, toward the outside of the layer the Zn content increases.

For the second group of alloys (Fig. 6c), it is observed in the vicinity of the substrate an area with an iron content of 7% which is specific to the δ phase (with an average iron content between 7 and 11.5%) (Ref 10).

3.2 Nanohardness

Structural variations in the hot-dip galvanized layer are causing a similar variation of its mechanical properties. An example of this is shown in Fig. 7. The microhardness and modulus of elasticity on sample 2.1, which had a galvanizing

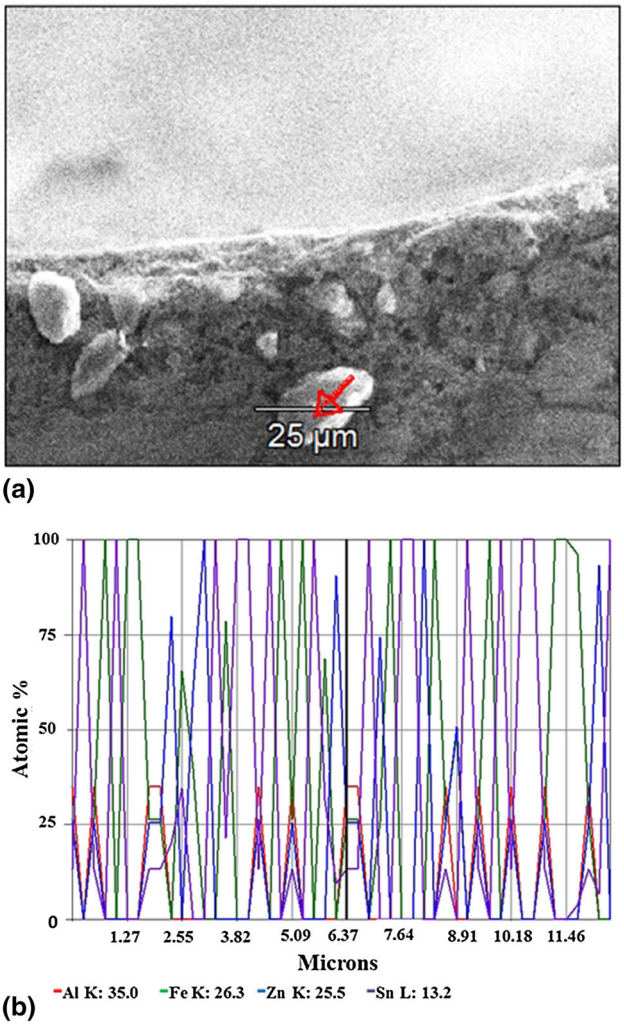

Fig. 5 (a) The microstructure of the deposited layer for the sample 1.2 galvanized at a temperature of 480 °C and immersed in the bath for 60 min. by electron microscope (accelerating voltage: 15 kV); (b) the variation of the composition in the arrow marked area (complex compound)

temperature of 480 °C and immersion time of 60 min., were determined by nanoindentation. The thickness of the deposited layer obtained in these conditions was about 90 microns. Measurements were taken in cross section from the edge of the layer to the steel substrate to highlight the difference in properties between the structural constituents. Very high variations in hardness are noted (up to 4 times higher in intermetallic compound areas than in solid solutions), associated with important variations of the modulus of elasticity. From the hardness surface mapping (Fig. 7c), one can observe that the intermetallic compounds (dark gray on the optical micrograph) are characterized by significantly higher hardness (lighter zones on the surface mapping graph), while the solid solution is represented by the dark regions.

3.3 Thermal Analysis

Thermal analysis was used as an assessment method of the dependence between the parameters of the galvanizing process (temperature, immersion time, the nature of the galvanizing

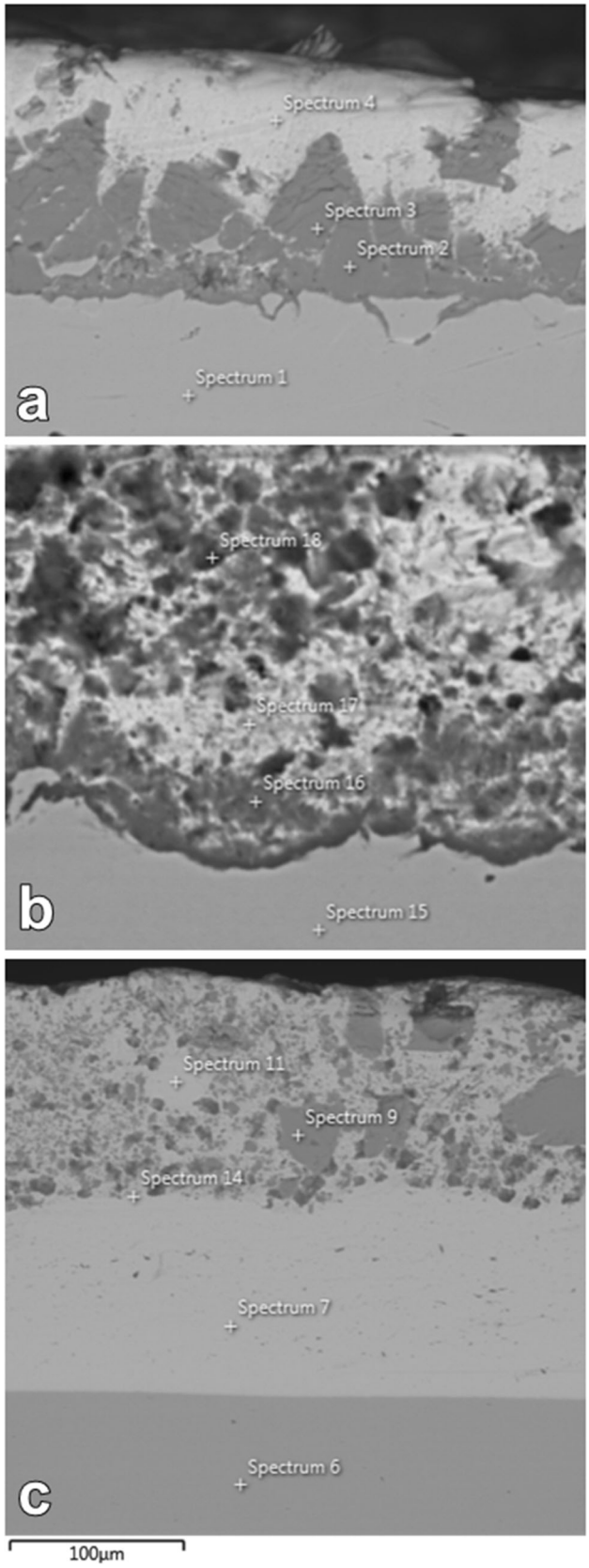

Fig. 6 (a) SEM micrograph for alloy 1.5 sample at a temperature of 450 °C immersed in the bath for 60 min; (b) SEM micrograph for alloy 1.2 sample at a temperature of 450 °C immersed in the bath for 60 min; (c) SEM/EDX analysis for alloy 2.5 sample at a temperature of 480 °C immersed in the bath for 60 min

Table 3 Chemical composition of various zones of the coatings and substrates (all in wt%)

Sample		Fe	C	Si	Al	Zn	Mn	O
1.5-450 °C	Spectrum 1	96.8	2.7	0.4	…	…	…	…
60 min	Spectrum 2	35.4	2.8	…	52.4	9.3	…	…
	Spectrum 4	0.8	5.4	…	…	93.8	…	…
1.2-450 °C	Spectrum 15	98.9	…	0.3	…	…	0.7	…
60 min	Spectrum 16	20.9	…	…	46.4	32.6	…	…
	Spectrum 17	3.3	…	…	17.3	79.4	…	…
	Spectrum 18	3.5	…	…	27.9	68.6	…	…
2.5-480 °C	Spectrum 6	96.6	3.4	…	…	…	…	…
60 min	Spectrum 7	7.1	4.3	…	1.4	85.3	…	2
	Spectrum 9	36.2	…	…	44.6	19.2	…	…
	Spectrum 11	7	…	…	3.7	89.3	…	…
	Spectrum 14	5.8	…	…	13.5	80.7	…	…

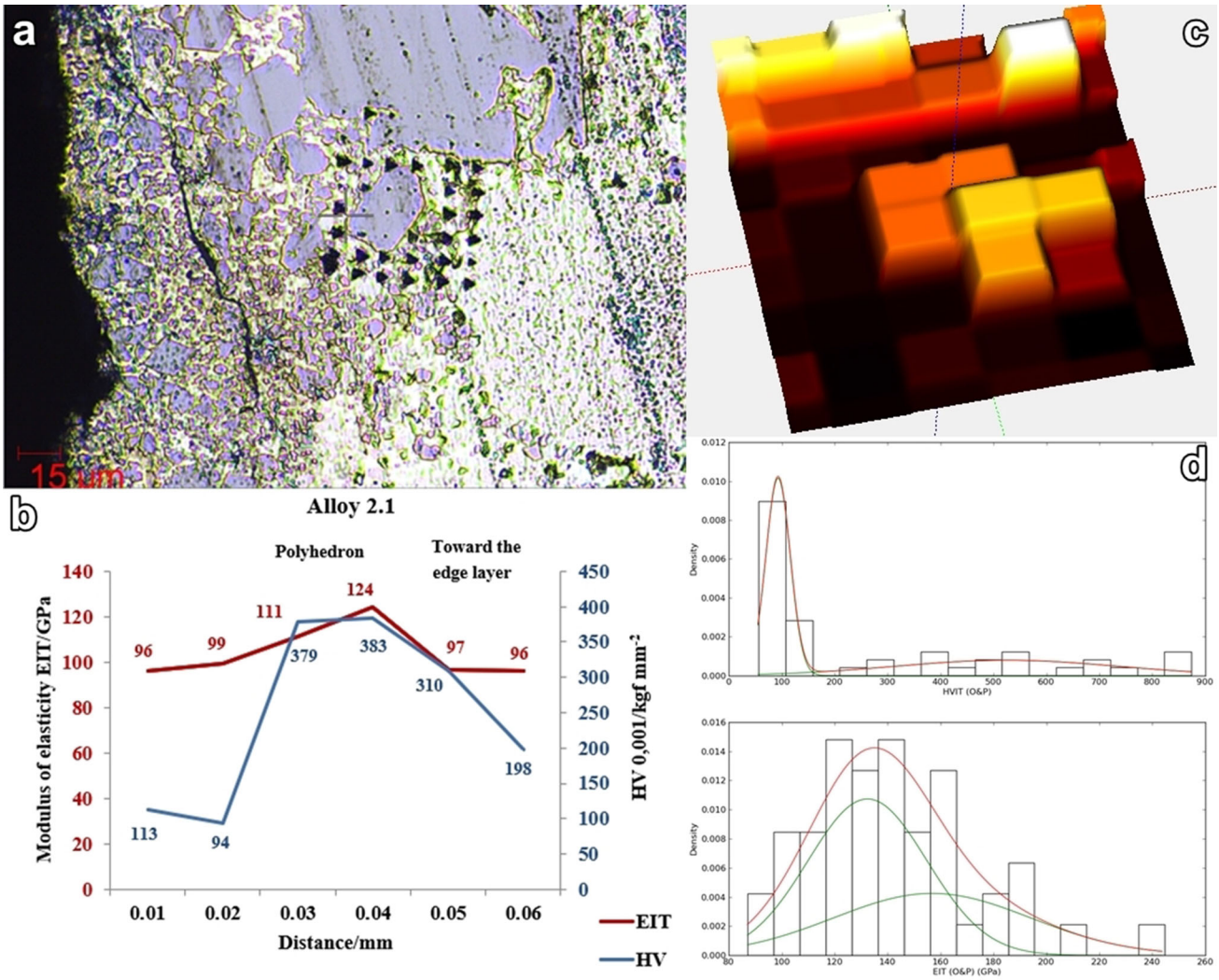

Fig. 7 Hardness and modulus of elasticity variation in the area of galvanic coating layer compounds in sample 2.1 (a) structure in the nanoindentation area; (b) hardness and modulus of elasticity variation on the nanoindentation area; (c) hardness surface mapping (darker regions signify softer phases); (d) hardness and elastic modulus phase distribution for two phases

alloy and the nature of the steel substrate) and the intensity of iron diffusion in the deposited layer. As previously discussed, this diffusion process is determinant for the structure and properties of the layer. This type of study is recommended due to the strong effect of iron on the critical phase transformation temperatures, in particular on the liquidus temperature in Zn-based alloys. Consequently, the observance of critical temperatures during heating and cooling (liquidus and solidus

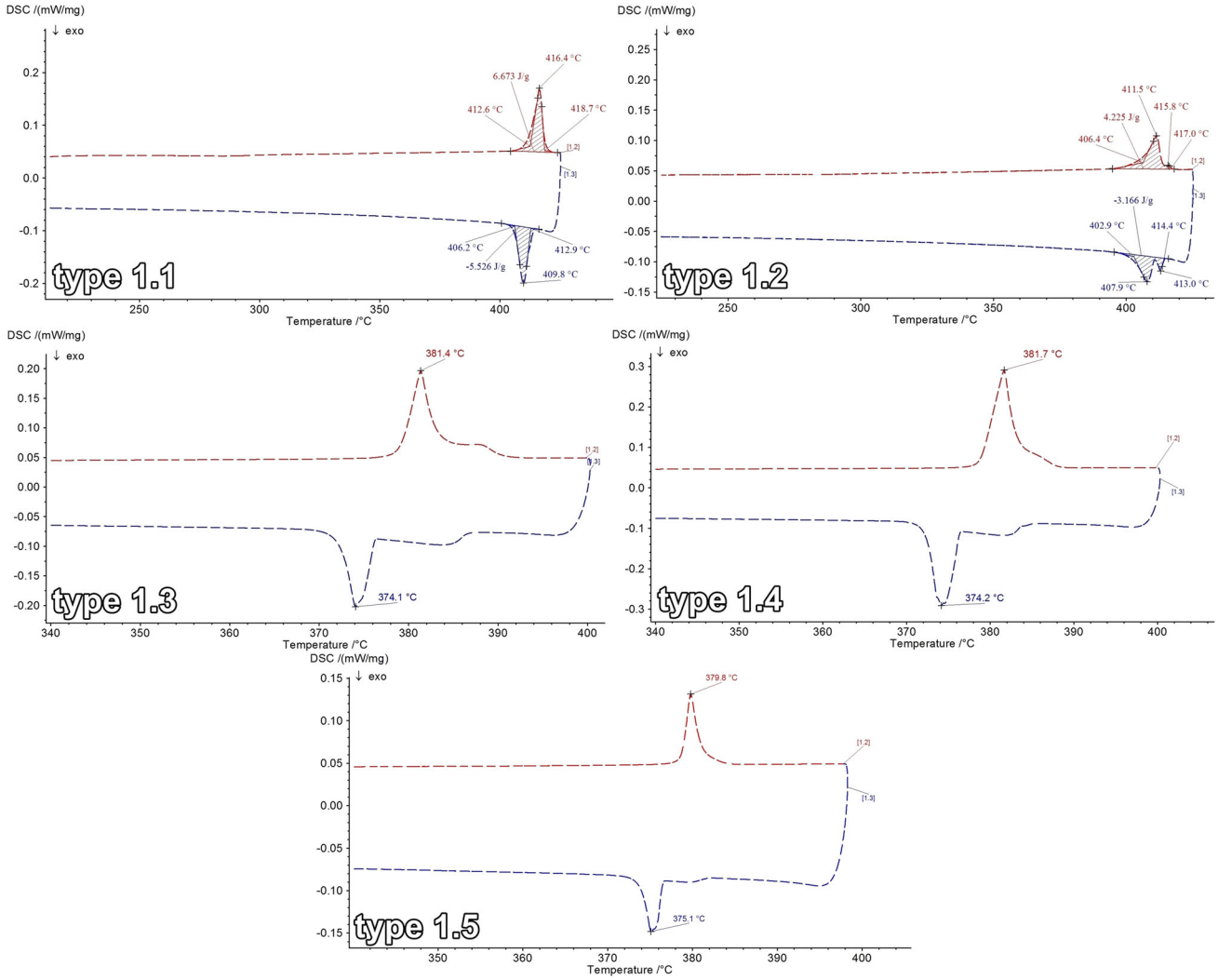

Fig. 8 Dependence between the chemical composition of the Zn-Al group alloys shown in Table 1 and the critical transformation temperatures (eutectic temperature, melting temperature and solidification temperature) at a temperature of 450 °C and a galvanizing bath immersion time of 60 min

temperature, eutectic temperature) should provide indirect information about the intensity of iron diffusion from the substrate in the coating deposited by hot-dip galvanization. The samples were subjected to differential scanning calorimetry studies, to determine the critical temperatures in the melting-solidification processes, also monitoring the possible solid-state phase transformations occurring in the coating.

The variation curves of thermal effects as function of temperature at a heating/cooling rate of 5 °C min^{-1} are shown in Fig. 8 and 9. In each of these figures, one can observe a certain order of the values of the melting temperatures (on the heating curves) and of the solidification temperatures (on the cooling curves) correlated with the deposition parameters.

From Fig. 8, one can observe that the critical temperatures are strongly correlated with the effect of Al on the galvanizing alloy (see the Zn-Al phase diagram, Fig. 3). For type 1.1 and 1.2 alloys with Al content $< 1\%$, the critical temperatures are higher than for alloys having Al $> 3\%$. Practically, the effect of decreasing the aluminum content in the galvanizing alloy overlaps with the increase in the iron content in the coating. It can be seen, however, that for alloys with relatively similar aluminum content, such as alloys 1.1 (0.868% Al) and 1.2 (0.713% Al), the positioning of melting temperatures is reversed in terms of the expectation extracted from the equilibrium diagram. This phenomenon can be attributed to the availability of the diffused iron in the galvanizing layer to participate in the formation of intermetallic compounds. The presence of aluminum favors this process, and thus, the solid solutions remain with a lower iron content, hence exhibiting a lower melting temperature.

In Fig. 9, one can observe that, with longer immersion periods, the critical temperature values are increasing, as well. This signifies an increase in the diffusion of iron in the respective alloys with increasing immersion time. Moreover, an increase in the iron content in the galvanized alloys causes an extension of their solidification range.

In order to establish more clearly the dependencies studied by thermal analysis, the critical temperature values were extracted from the DSC curves and were used to plot diagrams of linear regression, according to the variable deposition

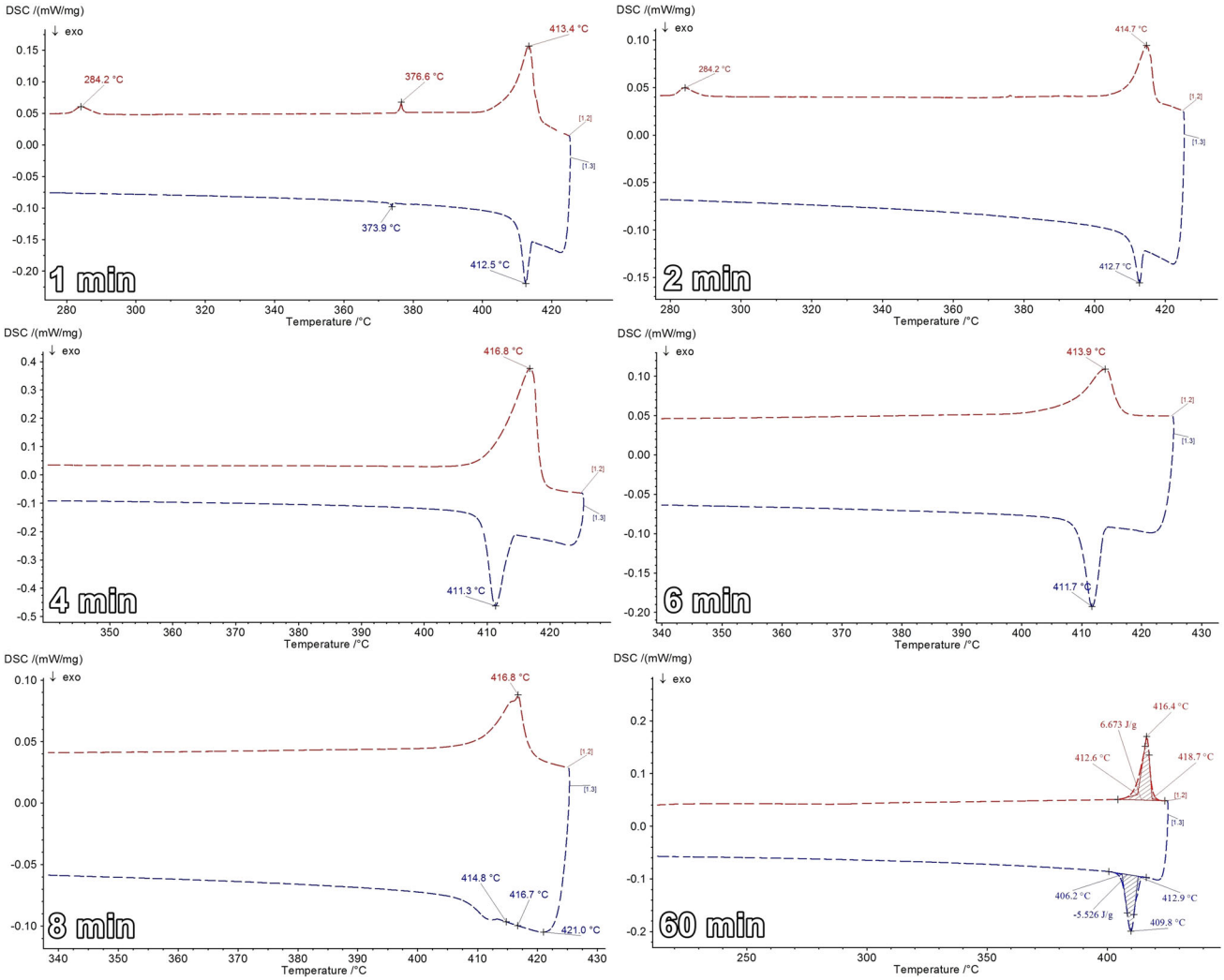

Fig. 9 Effect of the immersion time in the galvanizing bath on the critical temperatures for melting (during heating) and for solidification (during cooling) for Zn-Al binary alloy deposited layers with 0.868% Al, at a bath temperature of 450 °C

parameters (temperature, chemical composition and immersion time). The values for the critical transformation temperatures are shown in Table 4 (for Zn-Al alloys) and Table 5 (for Zn-Al-Ti-B alloys), and the representation of the dependence of these temperatures on the variable deposition parameters in the study is shown in Fig. 10.

In Fig. 10(a) and (b) are shown simple linear regressions for eutectic temperatures to heating (h) with a continuous line and with dashed line for eutectic temperatures at cooling (c). It can be observed that the eutectic temperature for heating is slightly higher than that at cooling. As expected, the eutectic temperature of the deposited layers' alloys depends very little on the variable deposition parameters. Basically, the variations can be framed within the limits of accuracy of the equipment used in the research (temperature accuracy = 0.1 K). This may be due to the fact that the thermal stability of the β solid solution is less influenced by the change in the percentage of iron in the alloy. The stability of the eutectic temperature can be explained due to the fact that this phase is essential for the eutectic transformation; hence, if the iron content does not have a significant effect on the stability of the β solid solution, no or slight temperature variation can be observed.

Figure 10(c) and (d) shows that in all cases an increase in the galvanizing bath temperature exacerbates the diffusion of elements from the steel substrate into the deposited layer. Because iron is the predominant element in this process of diffusion, the result is an increase in the melting and solidification temperatures of the alloy deposited in the layer. A higher intensity of this process is visible for Zn-Al-Ti-B alloys group, as compared with Zn-Al alloys (The lines in Fig. 10d have much higher slopes than those in Fig. 10c). This difference can be attributed to the small differences in the

Table 4 Transformation temperature values to heating and cooling for the Zn-Al alloy set at samples with a 60-min immersion time

			Heating, °C		Cooling, °C	
Alloy set 1	Al content, %	Galvanizing temp., °C	Eutectic temperature	Liquidus temperature	Eutectic temperature	Solidus temperature
1.1	0.868	450	…	416.4	…	409.8
		460	…	415.2	…	411
		470	…	416.2	…	409.8
		480	…	415.3	…	410.5
1.2	0.713	450	…	411.5	…	407.9
		460	…	415	…	410.5
		470	…	415	…	410.2
		480	…	415.1	…	411.1
1.3	3.79	450	381.4	389.2	374.1	385.1
		460	379.5	390.3	374.9	387.6
		470	380.8	390.8	374.5	386.2
		480	380.1	392.3	375.1	388.7
1.4	3.994	450	381.7	386.9	374.2	382.4
		460	380.5	389.8	374.6	386.1
		470	379.6	391.3	375.3	388.2
		480	380.7	…	374.5	394.9
1.5	5.276	450	379.8	383.9	375.1	381.5
		460	380.6	386.8	374.6	380.1
		470	380.3	387.1	374.6	384.6
		480	381	385.1	374.7	382.6

Table 5 Transformation temperature values to heating and cooling for the Zn-Al-Ti-B alloy set at samples with a 60-min immersion time

			Heating, °C	Cooling, °C
Alloy set 2	Al content, %	Galvanizing temp., %	Liquidus temperature	Solidus temperature
2.1	1.107	450	401.3	387.8
		460	416.3	…
		470	416.8	…
		480	416.8	410.6
2.2	2.137	450	…	383.6
		460	412.3	409.5
		470	417.2	…
		480	419.9	411.3
2.3	2.198	450	390.6	384.3
		460	415.8	…
		470	415.8	…
		480	417	…
2.4	2.518	450	390	386.7
		460	415.2	408
		470	416.1	…
		480	415.3	…
2.5	2.559	450	388.4	380.9
		460	415.9	411.1
		470	417.6	…
		480	417.9	…

composition of the steel substrates, but to a greater extent to the presence of Ti and B in the second group of alloys used as coatings.

The effect of the chemical composition of the galvanizing bath should be analyzed in correlation with the equilibrium diagram of the Zn-Al system (Fig. 3). The compositions presented herein are on the right side of the diagram and higher concentrations of Al translate to lower liquidus and solidus temperatures (Fig. 10e and f). From this point of view, there are significant differences between the two groups of alloys, as well. Thus, for Zn-Al group alloys (Fig. 10e) the observed effect of the chemical composition is the same in the studied cases. (The slopes of the lines are the same, being virtually parallel.) This indicates that the melting and solidification temperature changes are determined mainly by the action of other factors changed in the process (galvanization bath

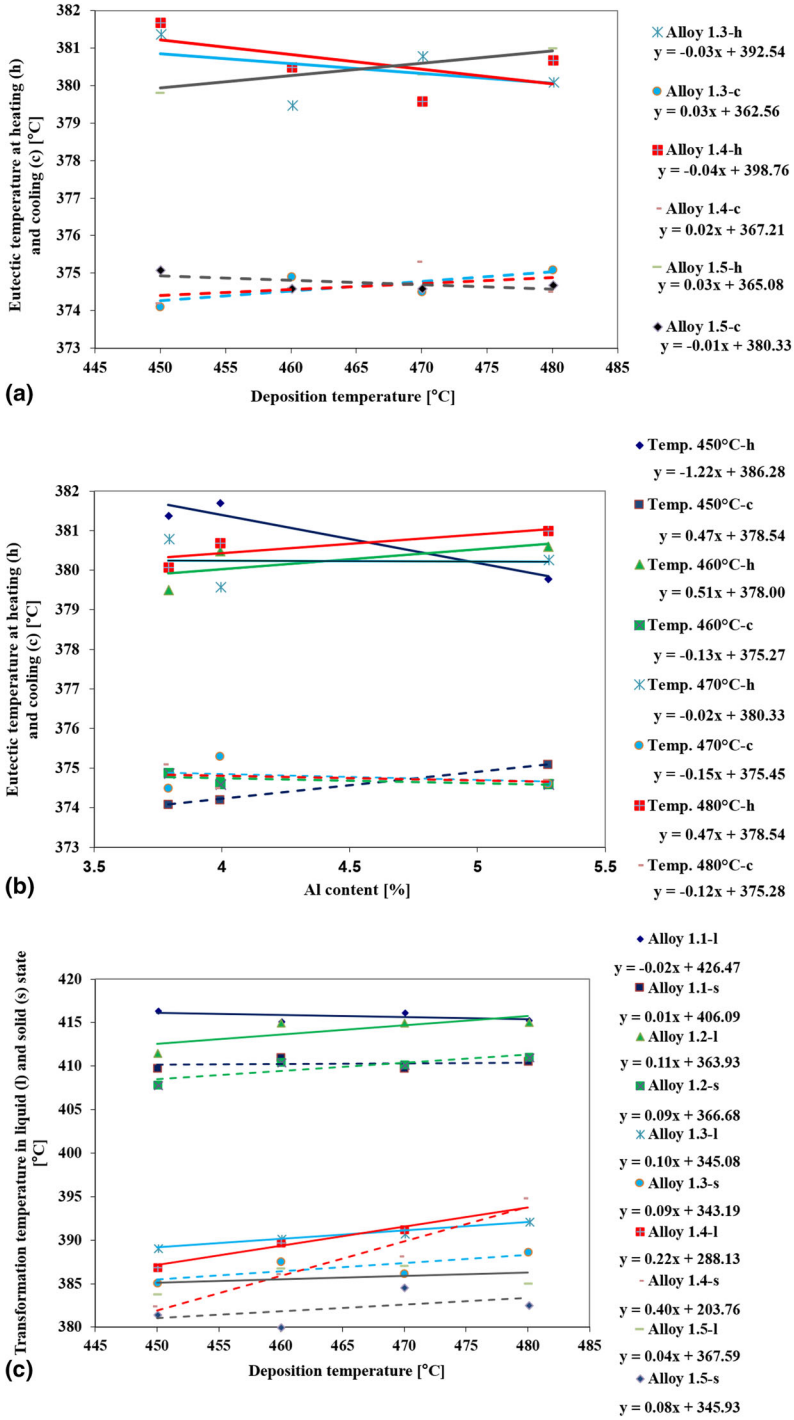

Fig. 10 (a) The dependence of the eutectic temperature at heating (h) and cooling (c) on the bath galvanizing temperature for the Zn-Al alloy, for 60 min. of immersion; (b) dependence of the eutectic temperature at heating (h) and cooling (c) on the chemical composition for the Zn-Al galvanizing alloy, at different temperatures of immersion in the galvanizing bath; (c) the dependence between the melting (l—continuous line) and solidification (s—dashed line) temperatures of the alloy from the layer deposited by the galvanization bath temperature for the Zn-Al group alloys. Bath immersion time = 60 min.; (d) the dependence between the melting (l—continuous line) and solidification (s—dashed line) temperatures of the alloy from the layer deposited by the galvanization bath temperature for the Zn-Al-Ti-B group alloys. Bath immersion time = 60 min.; (e) the dependence between the melting (l—continuous line) and solidification (s—dashed line) temperatures of the alloy from the layer deposited by the galvanization bath composition at different bath temperatures, for the Zn-Al group alloys. Bath immersion time = 60 min.; (f) the dependence between the melting (l—continuous line) and solidification (s—dashed line) temperatures of the alloy from the layer deposited by the galvanization bath composition at different bath temperatures, for the Zn-Al-Ti-B group alloys. Bath immersion time = 60 min.; (g) the dependence between the melting (l—continuous line) and solidification (s—dashed line) temperatures of the alloy from the deposited layer and the galvanization bath immersion time for the alloy from the Zn-Al system with 0.868% Al. Bath immersion temperature: 450 °C; (h) the variation in thickness of deposition layer for Zn-Al alloy type 1.1, as function of immersion period, 450 °C deposition temperature

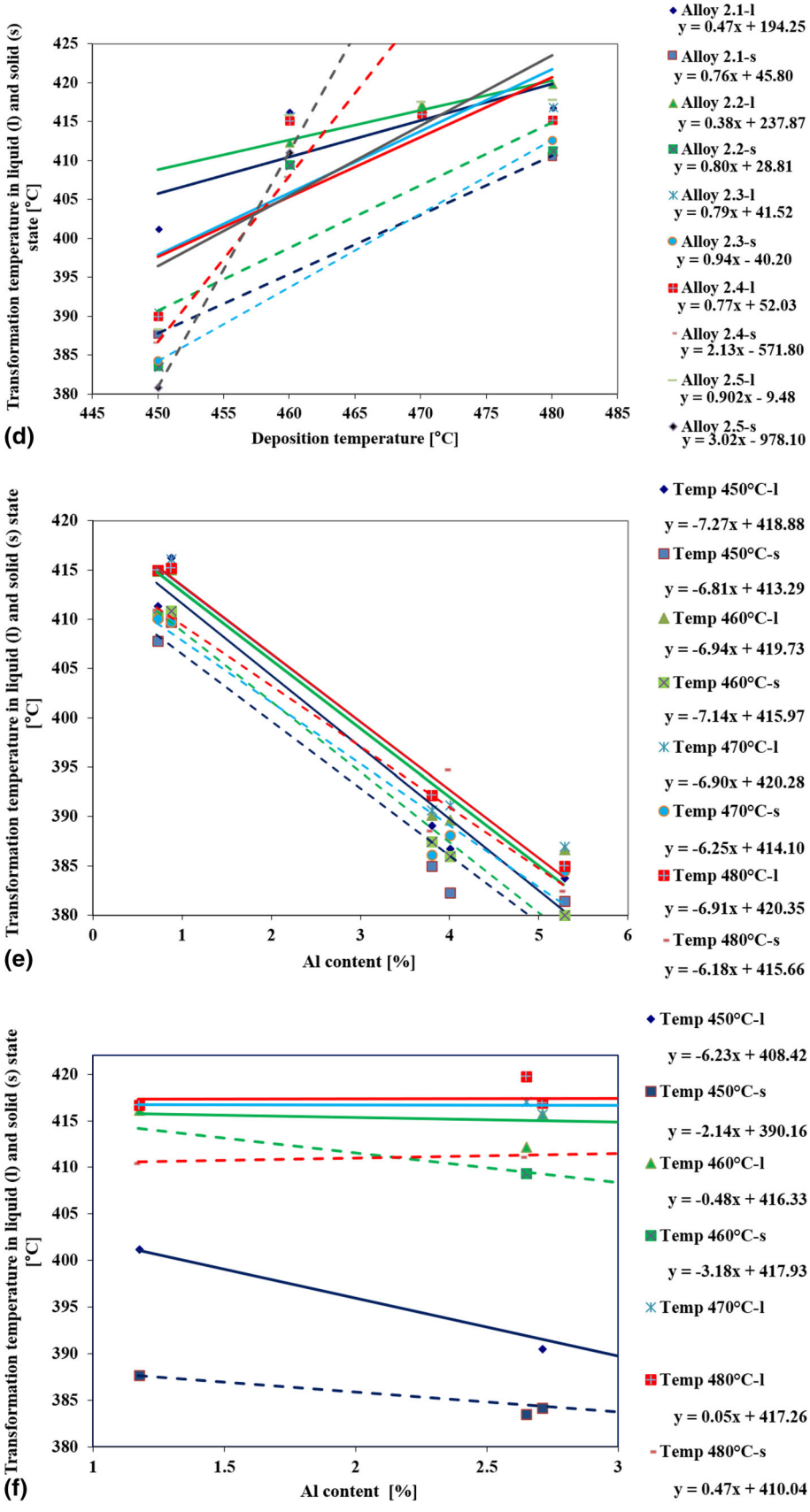

Fig. 10 continued

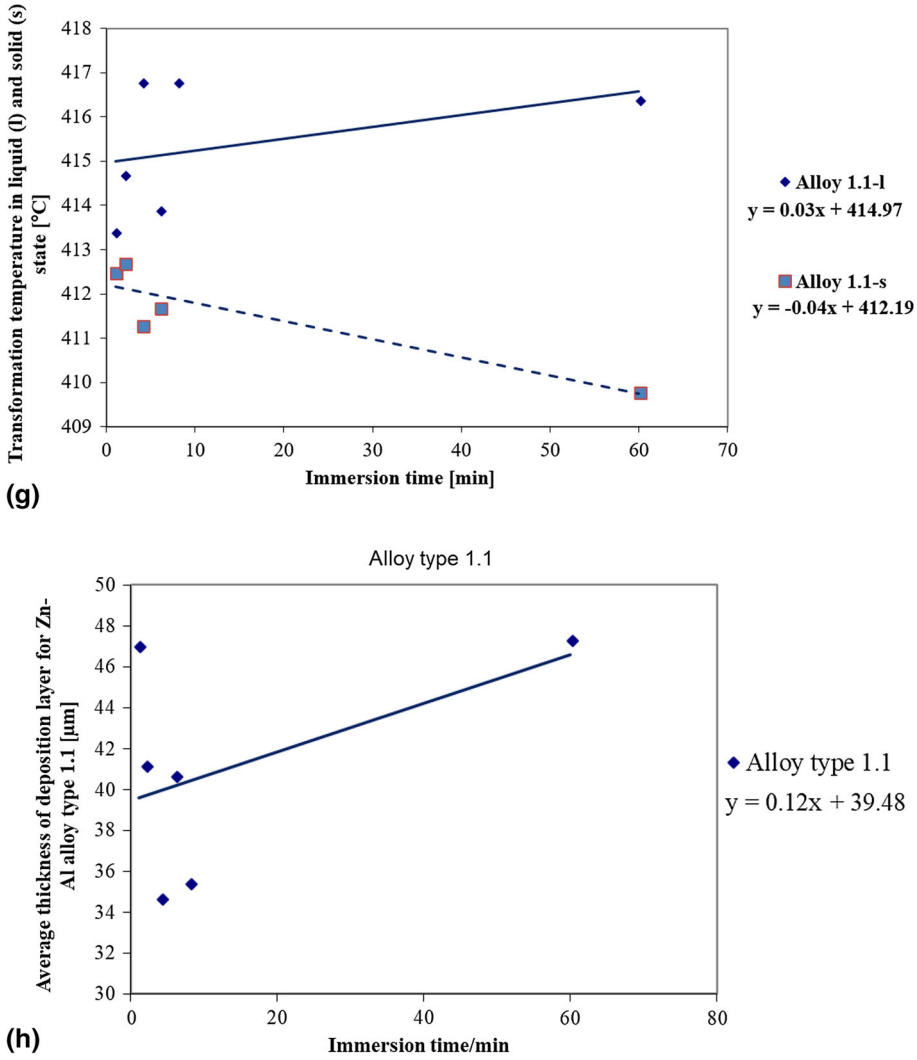

Fig. 10 continued

immersion temperature and time). But some observations made in the interpretation of Fig. 8 remain valid, on the effect of iron correlated with the modification of the composition of the galvanizing alloy.

Contrastingly, in the case of Zn-Al-Ti-B group alloys, important differences compared to the Zn-Al system can be observed (Fig. 10d). The higher the galvanizing bath temperature, the lesser the impact of the chemical composition of the bath on the iron diffusion from the substrate into the layer. However, this diffusion is more active than in the case of the Zn-Al system alloys (correlation between Fig. 10d and f). The presence of titanium and boron in the galvanizing alloy favors the formation of the intermetallic compounds which contain higher quantities of iron. Therefore, solid solutions in the structure contain less iron and their critical temperatures are less influenced by its presence.

The iron diffused in the coating causes the increase in the difference between the melting and solidification temperatures. This influence is shown in Fig. 10(g) for the type 1.1 coating alloy. This effect directly influences the solidification conditions of the deposited layer and consequently its thickness. The variation of the thickness as function of the immersion period is shown in Fig. 10(h). The higher the solidification layer range, the more can its thickness decrease, which could affect its durability in use. As the layer is thicker, denser and has higher tenacity properties, the durability of the coating should be improved.

4. Conclusions

Zn-based coatings were studied in terms of morphology, chemical composition, mechanical properties and thermal stability, in correlation with some variable deposition parameters (galvanizing bath chemical composition, immersion period, galvanizing temperature). The structure of the coatings is layered, with a specific order from the steel substrate to the outside. In these layers, the constituents are mixtures of solid solutions of Al in Zn (η and β) and intermetallic compounds.

Iron diffuses from the steel substrate into the coating layer and is distributed both in solid solutions and especially in intermetallic compounds.

The heterogeneous distribution of intermetallic compounds in the structure determines the non-uniformity of the mechanical properties of the layer. Two components can be noticed: intermetallic compounds which exhibit very high hardness, and significantly softer solid solutions.

Structural changes in the layers can be linked to the diffusion of iron from the steel substrate toward the coatings. For this reason, it is necessary to know the dependence between the parameters of the hot-dip galvanization process and the iron diffusion from the steel substrate in the deposited layer.

The degree of iron diffusion from the steel substrate in the deposited layer is difficult to quantify, primarily due to the non-homogeneous nature of the coatings. Thermal analysis allows a global appreciation of iron diffusion from the substrate to the layer, observing the changes that the iron's presence causes to the critical temperatures (melting, solidification, phase transformation).

Increasing the immersion time in the galvanizing bath and the bath temperature leads to an increase in iron diffusion in the coating layer. This phenomenon corresponds to an increase in the amount of intermetallic compounds, respectively, of iron content in the solid solutions.

The presence of some elements in the Zn alloy (Al, Ti, B) influences the distribution of the diffused iron in the layer, favoring the formation of the intermetallic compounds and less its dissolution in the solid solutions.

Among the elements in the coatings, aluminum covers a wider value range and consequently its effect on critical points (melting, eutectic, solidification) is the most significant. This is due to the fact that in the area of the aluminum contents (from 0.868 to 5.276% for alloy set 1 and from 1.107 to 2.559% for alloy set 2) the curves in the Zn-Al equilibrium diagram have very large slopes.

Increasing the iron content of the coating under the action of technological factors (increasing the immersion time and temperature in the galvanizing bath) leads to an increase in the solidification range of the alloy. This lowers the thickness of the deposited layer, thus reducing its durability in operation. When using complex alloys for hot-dip galvanizing, to obtain thicknesses and structures according to requirements, a more thorough control of the variable deposition parameters (bath temperature and composition, and immersion time) is required.

Acknowledgments

We hereby acknowledge the structural founds project PRO-DD (POS-CCE, O.2.2.1., ID 123, SMIS 2637, ctr. No 11/2009) for providing the infrastructure used in this work.

References

1. F. Delaunois and G. Guerlement, Installations sanitaires; l'acier galvanise a chaud au trempe devoile ses atouts, *Galvano-Organo*, 2007, **771**, p 26–29
2. G.M. Song and W.G. Sloof, Effect of Alloying Element Segregation on the Work of Adhesion of Metallic Coating on Metallic Substrate: Application to Zinc Coatings on Steel Substrates, *Surf. Coat. Technol.*, 2011, **205**, p 4632–4639
3. S.M.A. Shibli, R. Manu, and V.S. Dilimon, Effect of Nickel-Rich Barrier Layer on Improvement of Hot-Dip Zinc Coating, *Appl. Surf. Sci.*, 2005, **245**, p 179–185
4. M.N. Avettand-Fenoel, N. David, G. Reumont, J.M. Fiorani, M. Vilasi, and P. Perrot, Assessment of the Fe-Sn-Zn Phase Diagram at 450°C. Application to the Batch Galvanizing, *J. Therm. Anal. Calorim.*, 2007, **90**, p 329–332
5. C.S. Che, J.T. Lu, G. Kong, Q.Y. Xu, and J.H. Chen, Influence of Silicon in Steels on Galvanized Coatings, *Acta Metall. Sin.*, 2006, **19**, p 85–90
6. K. Tachibana, Y. Morinaga, and M. Mayuzumi, Hot Dip Fine Zn and Zn-Al Alloy Double Coating for Corrosion Resistance at Coastal Area, *Corros. Sci.*, 2007, **49**, p 149–157
7. J.B. Nasr, A. Snoussi, C. Bradai, and F. Halouani, Optimization of Hot-Dip Galvanizing Process of Reactive Steels: Minimizing Zinc Consumption Without Alloy Additions, *Mater. Lett.*, 2008, **62**, p 3328–3330
8. J.B. Nasr, A. Snoussi, C. Bradai, and F. Halouani, Effect of the Withdrawal Speed on the Thickness of the Zinc Layer in Hot Dip Pure Zinc Coatings, *Mater. Lett.*, 2008, **62**, p 2150–2152
9. Q. Luo, J.L. Chen, Y. Li, F. Yang, Q. Li, Y. Wu, J.Y. Zhang, and K.C. Chou, Experimental Study and Thermodynamic Assessment of the Al-Fe Rich Side of the Al-Zn-Fe System at 300 and 550°C, *Comput. Coupling Phase Diagr. Thermochem.*, 2012, https://doi.org/10.1016/j.calphad.2012.02.007
10. P. Pokorny, J. Kolisko, L. Balik, and P. Novak, Reaction Kinetics of the Formation of Intermetallic Fe-Zn During Hot-Dip Galvanizing of Steel, *Metallurgy*, 2016, **55**, p 111–114
11. M. Demirtas, G. Purcek, H. Yanar, Z.J. Zhang, and Z.F. Zhang, Effect of Chemical Composition and Grain Size on RT Superplasticity of Zn-Al Alloys Processed by ECAP, *Lett. Mater.*, 2015, **5**(3), p 328–334
12. P. Pokorny, J. Kolisko, L. Balik, and P. Novak, Description of Structure of Fe-Zn Intermetallic Compounds Present in Hot-Dip Galvanized Coatings on Steel, *Metallurgy*, 2015, **54**(4), p 707–710